

Multiregion Bilinear Convolutional Neural Networks for Person Re-Identification

Evgeniya Ustinova,^{1,*} Yaroslav Ganin,^{1,†} and Victor Lempitsky^{1,‡}

¹*Skolkovo Institute of Science and Technology
Skolkovo, Moscow, Russia*

In this work we explore the applicability of the recently proposed convolutional neural net architecture, called Bilinear CNN, and its new modification that we call Multiregion Bilinear CNN to the person re-identification problem. Originally, Bilinear CNNs were introduced for fine-grained classification and proved to be both simple and high-performing architectures. Bilinear CNN allows to build an orderless descriptor for an image using outer product of features produced from two separate feature extractors. Based on this approach, Multiregion Bilinear CNN, apply bilinear pooling over multiple regions for extracting rich and useful descriptors that retain some spatial information.

We show that when embedded into a standard “siamese” architecture, bilinear CNNs and in particular their multiregion variants can improve re-identification performance compared to standard CNNs and achieve state-of-the-art accuracy on the largest person re-identification datasets available at the moment, namely CUHK03 and Market-1501.

I. RELATED WORK

A. Deep CNNs for Re-Id

Several CNN-based methods for person re-identification have been proposed recently [1, 12–14]. Yi *et al.*[1] introduce “siamese” architecture consisting of two CNNs, connected by the similarity layer (cosine similarity is used). Two images are processed independently in the network, and only their final representations are connected in the similarity calculation step. In [1] special architecture specific to pedestrian images is proposed. Each of the two “siamese halves” includes three independent sub-networks, in which three overlapping parts of person images are processed separately (head and upper torso, torso, legs and lower torso). This is done in order to take into account different statistics of textures, shapes, and pose changing in different parts of the image.

Differently to [1], [12] and [13] learn classification networks that can categorize a pair of images as either depicting the same subjects or different subjects. In both approaches, the two images are fed into the network, and the difference in their mid-level representation is processed by additional special layers (Patch matching in [12] and cross-input neighbourhood difference in [13]). After that, extra convolutional and inner product layers are applied to the combined representation of the pair of images. Finally, the classification for the pair of images is performed using softmax layer. The proposed deep learning approaches [1, 12, 13], while competitive, do not clearly outperform more traditional approaches based on “hand-engineered” features [9, 17].

When searching for matches in a dataset, the methods proposed in [12], [13] and [14] need to process pairs that include the query and every image in the dataset, and hence cannot directly utilize fast retrieval methods based on Euclidean and other simple distances. Here we aim at the approach that can learn per-image descriptors and then compare them with cosine similarity measure. This justifies starting with the architecture proposed in [1] and then modifying it by inserting new layers.

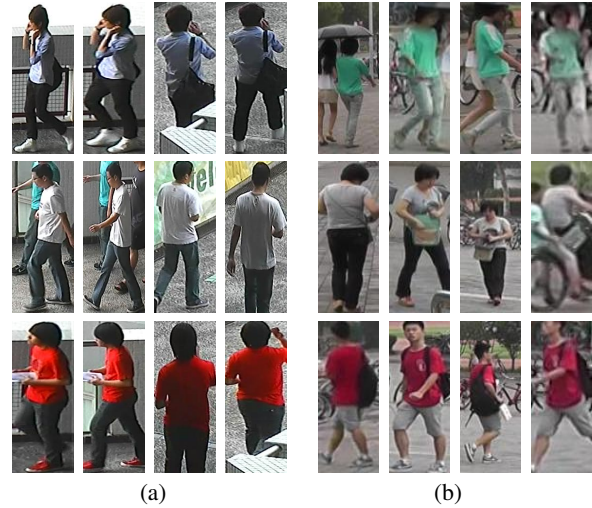


FIG. 1: (a) - sample images of the CUHK03 dataset [12]. Each person is captured by two cameras. There are six camera views in total. Each row corresponds to a person. First two images in a row are samples of first camera view for a person, 3th and 4th images are from the second camera view for a person. All the images in this paper are better viewed in color. (b) - sample images of the Market-1501 dataset [15]. Each row corresponds to a person, different camera views are shown for each identity. Each person is captured by at most six cameras.

B. Bilinear CNNs

Bilinear convolutional networks (B-CNN), introduced in [18] achieved state-of-the-art results for a number of fine-grained recognition tasks, and have also shown potential for face verification [19]. B-CNN consists of two CNNs (where the input of these two CNNs is the same image) without fully-connected layers. The outputs of these two streams are combined in a special way via bilinear pooling. In more detail, the outer product of deep features are calculated for each spatial location, resulting in the quadratic number of feature maps, to which sum pooling over all locations is then performed. The resulting orderless image descriptor is then used in subsequent processing steps. For example, in [18] and [19] it is normalized and fed into the softmax layer for classification. An intuition given in [18] is that the two CNN streams combined by bilinear operation may correspond to part and texture detectors respectively. This separation may facilitate localization when significant pose variation

* evgeniya.ustinova@skolkovotech.ru

† ganin@skolkovotech.ru

‡ lempitsky@skoltech.ru

is present without the need for any part labeling of the training images.

II. THE APPROACH

The difficulty of person re-identification problem lies in several factors of person appearance variation, including lighting changes, different poses, different view points. Many challenges of person re-identification are shared with the fine-grained recognition task: one person can look very differently when captured by different cameras, and different persons can look similar if they wear similar clothes and can only be distinguishable based on a small outfit element. Moreover, person re-identification and fine-grained classification have already been approached with related methods [10, 18]. Our solution combines the state-of-the-art method for person re-identification (Deep Metric Learning [1]) and the state-of-the-art fine-grained recognition method (bilinear CNN [18]). A simple modification (multiregion pooling) boosts the performance of this combination significantly.

A. Multiregion Bilinear Model

Bilinear CNNs are motivated by the specialized pooling operation that aggregates the correlations across maps coming from different feature extractors. The aggregation however discards all spatial information that remains in the network prior to the application of the operation. This is justified when the images lack even loose alignment (as e.g. in the case of the birds dataset), however is sub-optimal in our case, where person detector ensures that there is some loose geometric alignment between images. Therefore we modify bilinear layer and replace it with the *multiregion bilinear layer*, which allows us to retain some of the geometric information. Our modification is, of course, similar to many other approaches in computer vision, notably to spatial pyramids of [28].

Similar to [18], we introduce bilinear model for image similarity as follows:

$\mathcal{B} = (f_A, f_B, \mathcal{P}, \mathcal{S})$, where f_A and f_B are feature extractor functions, \mathcal{P} is the pooling function, \mathcal{S} is the similarity function. The feature function takes an image \mathcal{I} at location \mathcal{L} and outputs the feature of determined dimension \mathcal{D} (unlike [18], we use vector notation for features for simplicity): $f : \mathcal{I} \times \mathcal{L} \rightarrow \mathcal{R}^{1 \times \mathcal{D}}$. In this work, two convolutional CNNs (without fully-connected layers) serve as the two feature extractors f_A and f_B .

For each of the two images in the pair at each spatial location, the outputs of two feature extractors f_A and f_B are combined using the bilinear operation [18]:

$$bilinear(l, im, f_A, f_B) = f_A(l, im)^T f_B(l, im), l \in \mathcal{L}, im \in \mathcal{I} \quad (2.1)$$

In this way, we compute the bilinear feature vector for each spatial location l of the image im . If the feature extractor f_A outputs local feature vectors of size M and the f_B feature extractor outputs feature vectors of size N , their bilinear combination will have size $M \times N$, and for notational simplicity we assume that the output of bilinear operation is reshaped to $MN \times 1$.

We then suggest to aggregate obtained bilinear features across locations situated in predefined set of image regions: r_1, \dots, r_R ,

where R is number of chosen regions. After such pooling, we get the pooled feature vector for each image region i (as opposed to the feature vector that is obtained in [18] for the whole image):

$$\phi_{r_i}(im) = \phi(im_{r_i}) = \sum_{l \in r_i} bilinear(l, im, f_A, f_B) \quad (2.2)$$

In order to get a descriptor for image im , we combine all region descriptors into a matrix of size $R \times MN$:

$$\phi(im) = [\phi_{r_1}(im)^T; \phi_{r_2}(im)^T; \dots; \phi_{r_R}(im)^T]. \quad (2.3)$$

This matrix can be turned into a vector descriptor by reshaping. Alternatively, some transforms can be applied beforehand. Formally, such additional transforms can be incorporated into the similarity function \mathcal{S} . For example, fully connected layer performs additional transform in our architecture. Note, that for some types of transforms (for example, for convolution) spatial order of pooling regions should be preserved.

In our experiments, we simply used the grid of equally-sized non-overlapping patches as a set of pooling regions, and concatenate the matrix columns in (2.3) into a single global descriptor. Note, that corresponding receptive fields of the input image will still be overlapping. The scheme of Multiregion Bilinear CNN architecture is shown in figure 2a.

B. Learning the model

We now discuss the combination of Deep Metric Learning (DML) and Bilinear CNN (B-CNN) architectures. As in DML [1], we use the siamese architecture, where two pedestrian images are fed into the identical neural networks. The two output vectors can then be regarded as the descriptors of the two input images. Similarity and cost function value are then calculated for obtained descriptors. Similar to [1], we use cosine similarity function and the Binomial Deviance loss function:

$$J_{dev} = \sum_{i,j \in I} w_{i,j} \ln(\exp^{-\alpha(s_{i,j} - \beta)m_{i,j}} + 1), \quad (2.4)$$

where I is the set of training image indices, and $s_{i,j}$ is the similarity measure between i th and j th images (i.e. $s_{i,j} = \cos(x_i, x_j)$).

Furthermore, $m_{i,j}$ and $w_{i,j}$ are the learning supervision and scaling factors respectively:

$$m_{i,j} = \begin{cases} 1, & \text{if } (i, j) \text{ is a positive pair} \\ -1, & \text{if } (i, j) \text{ is a negative pair} \end{cases}$$

$$w_{i,j} = \begin{cases} \frac{1}{n_1}, & \text{if } (i, j) \text{ is a positive pair} \\ \frac{1}{n_2}, & \text{if } (i, j) \text{ is a negative pair} \end{cases}, \text{ where } n_1 \text{ and } n_2 \text{ are the number of positive and negative pairs in the training set (or training batch) correspondingly, } \alpha, \beta \text{ are hyper-parameters.}$$

Following the original architecture [1], we use the two convolution layers with 64 output feature maps (filter size of the first one is 7×7 , and of the second one is 5×5), followed by the rectified linear (ReLU) non-linearity and max pooling with the kernel size of two pixels and the stride of two pixels. Also following [1], we use separate sub-networks for the three parts of pedestrian images (head and upper torso, torso, legs and lower

torso) to take into account different semantic nature of the three parts. As in [1], we have the weights of the first convolution layers shared for the three sub-networks.

We incorporate the multiregion bilinear operation (2.3) into the architecture in the following way: instead of using one sub-network for each image part, we use two feature extractors with the same architecture described above. The outputs are combined by the multiregion bilinear operation (2.3) after the second convolution. Three bilinear outputs for each of the image parts are then concatenated and turned into a 500-dimensional image descriptor by an extra fully connected layer. The overall scheme of Multiregion Bilinear DML net for each of the two siamese sub-networks used in this work is shown in figure 2b.

III. EXPERIMENTS

A. Datasets and evaluation protocols

We investigate the performance of DML method and its Bilinear variant (figure 2) for two re-identification datasets: CUHK03 [12] and Market-1501 [15]. The CUHK03 dataset includes 13,164 images of 1,360 pedestrians captured from 3 pairs of cameras. Each identity is observed by two cameras and has 4.8 images in each camera on average. The two versions of the dataset are provided: *CUHK03-labeled* and *CUHK03-detected* with manually labeled bounding boxes and automatically detected ones accordingly.

Following [12], we use Cumulative Matching Characteristic curve (CMC) metric to report our results. The evaluation protocol accepted for the CUHK03 is the following: 1,360 identities are split into 1,160 identities for training, 100 for validation and 100 for testing. At test time single-shot CMC curves are calculated. We use one split for choosing architecture and parameters (figure 4) and five random splits to calculate the resulting average CMC (figures 3, 5). Some sample images of CUHK03 dataset are shown in figure 1a.

We also report our results on the Market-1501 (1b) dataset, introduced in [15]. This dataset contains 32,643 images of 1,501 identities, each identity is captured by at most six cameras and by at least two cameras. The dataset is randomly divided into the test set of 750 identities and the train set of 751 identities. We split training set for train and validation into 700 and 51 identities correspondingly. For each identity in the test set one image in each camera is selected and used as a query. Manually drawn bounding boxes are used for query images, and automatically detected ones for training images as well as for the gallery images in the test set. Market-1501 also includes "distractor" images that correspond to false detections, which makes evaluation on the dataset even more realistic and challenging. As in [15], we also evaluate the re-identification performance using the multi-shot protocol (multiple images from the same camera are present for each identity in the gallery set) for both datasets. Following [15], we also demonstrate results with the multi-query approach, when all images of a person from one camera are used as a query, instead of using only one randomly chosen image as in the standard and the multi-shot protocols.

B. Architectures evaluated

Here we list the three architectures we evaluate in this paper. We use DML architecture from [1] as the baseline method. We also evaluate the baseline Bilinear DML ("*B-DML*") architecture where bilinear features are pooled over all locations for each of the three image parts. This corresponds to the formula (2.3), where whole image is used for pooling. Finally, we present the results for Multiregion Bilinear CNN ("*MR B-DML*") introduced in this paper (figure 2).

Implementation details As in [1], we form training pairs inside each batch consisting of 128 randomly chosen training images (from all cameras). The label for each training pair is assigned accordingly to identity numbers (+1 for the same identity, -1 for different identities). The training set is shuffled after each epoch, so the network can see many different image pairs while training. All images are resized to height 160 and width 60 pixels. Binomial Deviance (2.4) is used as loss function, and its parameters, as in [1], are set to $\alpha = 2$, $\beta = 0.5$ and $C = 2$. Cosine similarity is used to compute the distance between a pair of image descriptors.

We train networks (DML and the variants of B-DML) with the weight decay rate of 0.0005. The learning rate is changing according to "step" policy, the initial learning rate is set to 0.001 and it is multiplied by 0.1 when the performance on the validation set stops improving (50,000 iterations for CUHK03, and 40,000 for Market-1501). The dropout layer with probability of 0.5 is inserted before the fully connected layer. DML and B-DML are learned for 90,000, and MR B-DML nets are learned for 55,000 iterations on CUHK03 and Market-1501. B-DML and MR B-DML networks are initialized by the weights of the DML net trained on the same dataset for 60,000 iterations¹.

C. Variations of the Bilinear CNN architecture

We started our experiments with comparing the performance of the baseline DML method and the bilinear modification B-CNN. Experiments showed that for the CUHK03-labeled dataset, the DML network outperformed all the B-DML variants, while for the CUHK03-detected version the situation was reversed: results for B-DML were better (see figure 4). This confirms that the latter scenario is more beneficial for the bilinear networks due to their ability to handle pose variations and/or lack of registration.

We also experimented with different initializations of two feature extractor CNNs, trying to benefit from segmentation/detection pre-training. Initializing the two feature extractors identically with the parameters of the baseline DML network appeared to be the best option. We also observed that without such pre-training, the performance of the bilinear architecture drops noticeably. Thus, we use this initialization in all subsequent experiments.²

¹ We tried learning baseline for more iterations (because the total number of learning iterations for Bilinear nets, including pretraining, is more than 90,000) and also decreasing the learning rate later. However this did not improve the baseline DML performance.

² See supplementary material for the details.

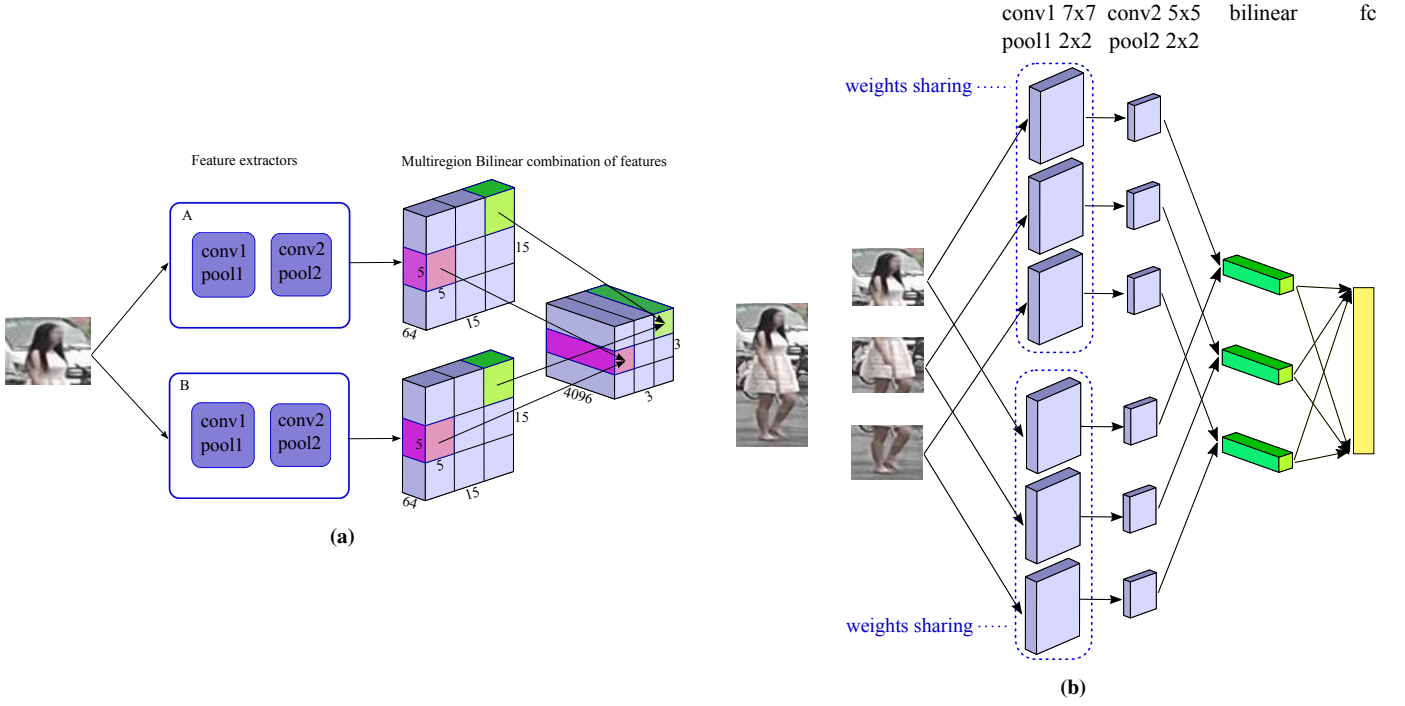


FIG. 2: Introduced architecture (a) - multiregional bilinear sub-network used for each of the three parts of the input image, (b) - overall Mutiregion Bilinear DML architecture. See text for more detailed information.

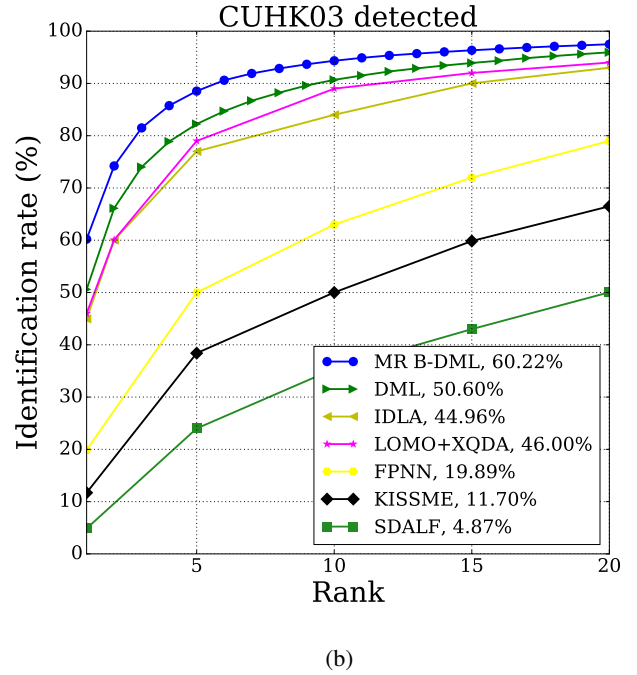
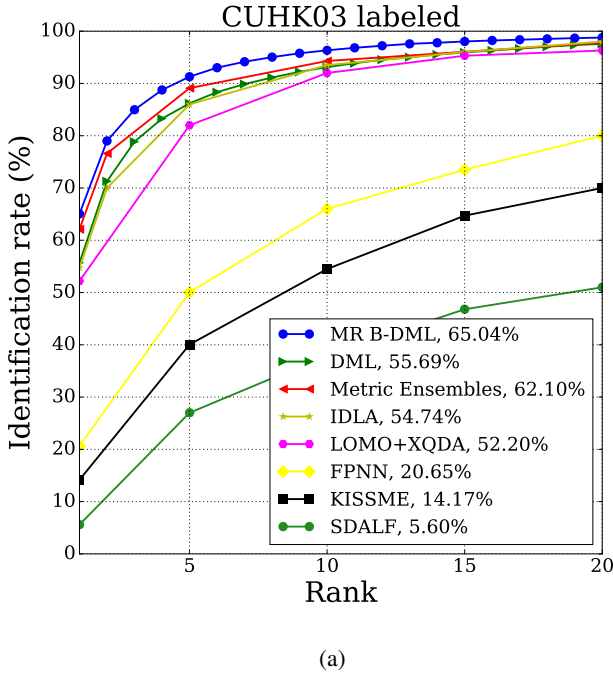


FIG. 3: Single-shot results (CMC) of different methods for CUHK03 (a) - labeled, (b) - detected. Multiregion Bilinear DML outperforms the state-of-the-art methods on both versions of CUHK03.

Before adding multiregion pooling, we tried to improve the performance of B-DML CNN in some simpler ways. We observed that in our case pooling across all locations in the Bilinear DML network causes the dramatic decrease of the number of parameters compared to the well-tuned DML architecture (21,916,608 parameters in the baseline DML network vs 6,777,216 parameters in the Bilinear DML network). Hence, we

decided to check if the increase in the number of parameters of the B-DML network will improve its performance, and tried two ways to make the number of parameters of the B-DML network to match the number of parameters of the original baseline DML model.

First, we tried to insert additional fully connected layer with 1,689 output channels followed by ReLU non-linearity after the

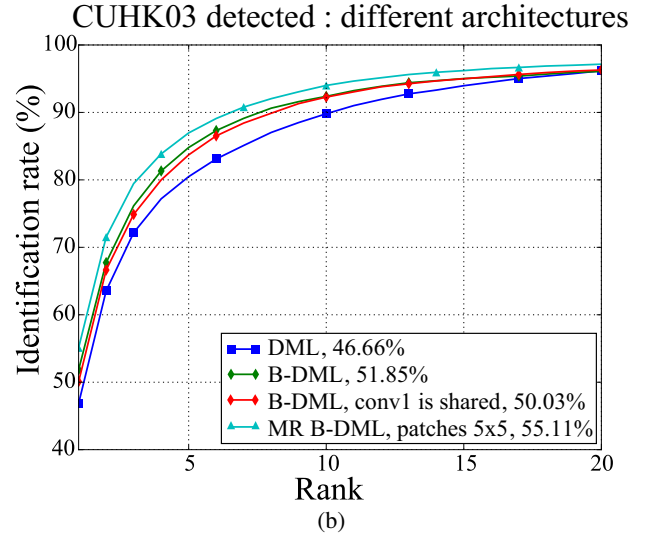
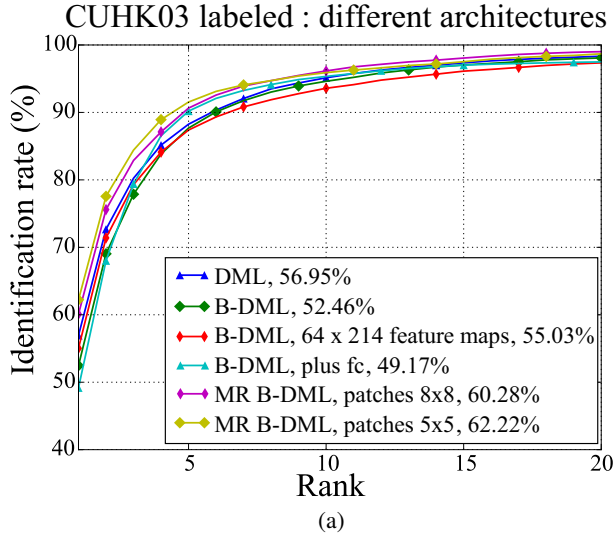


FIG. 4: Single-shot results (CMC) of different architectures for CUHK03 (a) – CUHK03-labeled, (b) – CUHK03-detected (single-shot CMC). DML is compared to B-DML (pooling of bilinear features is done across all locations) and the MR B-DML proposed in this work (pooling of bilinear features is done across locations within certain patches). Several variations for B-DML and MR B-DML discussed in the text are compared.

bilinear operation in the B-DML network. Second, we tried to increase the number of feature maps in the second convolution layer in one of the two feature extractors from 64 to 214. These experiments were carried out on the CUHK03-labeled dataset. As shown in figure 4a, B-DML net with additional fully connected layer (*B-DML, plus fc*) outperforms baseline DML and B-DML networks for a number of rank values between 3 and 15, but it shows much worse identification rate for rank 1. On the other hand, the B-DML network with the increased number of feature maps for one of the two feature extractors (*B-DML, 64x214*) performed better than the baseline B-DML network only for ranks 1-4. And it was still worse than DML for all rank values.

We also showed that two separate feature extractors are important for the performance of the bilinear architecture: we tried to share the first convolution layer for the two feature extractors, which resulted in lower identification rate in comparison with the baseline B-DML net for all rank values.

D. Adding multiregion pooling

Finally, we have added the multiregion pooling and this gave considerable performance boost for all rank values (figure 4). The improvement is consistent for both variants of CUHK03. The experiments were conducted with the baseline DML initialization. Without such pre-training, performance of Multiregion Bilinear DML drops approximately by 3% at rank 1. Figure 4 also shows that the performance for Multiregion Bilinear DML net with pooling within patches of size 5×5 (MR B-DML, patches 5×5) noticeably outperforms Multiregion Bilinear DML with pooling within patches of size 8×8 for the first 7 ranks, and for the other ranks values it is only slightly worse.

It also should be mentioned, that Multiregion Bilinear DML may have much more parameters than the baseline DML and the B-DML, because of the increasing size of the matrix inside the fully connected layer. We however observed no performance improvement for the baseline DML with the increased number

TABLE I: Rank-1 for multi-shot experiments on CUHK03 and Market-1501. Mean average precision is reported for the Market-1501 dataset.

Methods	CUHK03	CUHK03	Market-1501	
	labeled r = 1	detected r = 1	r = 1	mAP
Zheng <i>et al.</i> [15], MQ, max		24.33	47.25	21.88
Multiregion Bilinear DML (ours)	71.98	67.96	45.58	26.11
Multiregion Bilinear DML, MQ, max (ours)	79.80	74.4	53.62	30.76
Multiregion Bilinear DML, MQ, avg (ours)	80.60	76.2	56.59	32.26

of parameters, which can testify to real usefulness of bilinear features.

E. Multi-shot results

Following [15], we also evaluated our method using multi-shot re-identification protocol. As expected, multi-shot results are much higher than single-shot for both versions of CUHK03. Using several images for a query (multi-query protocol) improves the results further for both CUHK03 and Market-1501.

As in [15], we performed multi-shot evaluation with multiple queries, using two pooling approaches: 1) average pooling, when descriptors of several queries are pooled into one by averaging, 2) max-pooling, when resulting descriptor consists of maximum values of the query descriptors in each dimension. Our experiments showed that pooling strategies for queries improve performance significantly, which can be explained by the fact, that pooled descriptors incorporate information about different poses present in multiple query images. Average pooling strategy turned out to be more effective for our descriptors than max pooling. It is only slightly better than max-pooling for CUHK03 (see figure 5) and noticeably better for Market-1501 (see figure 6).

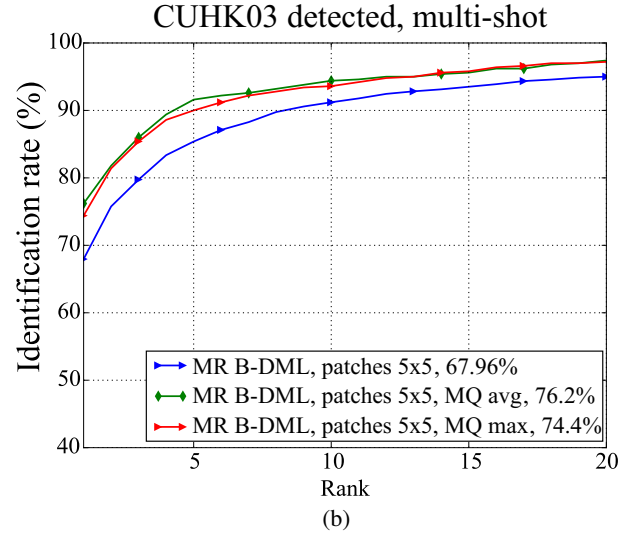
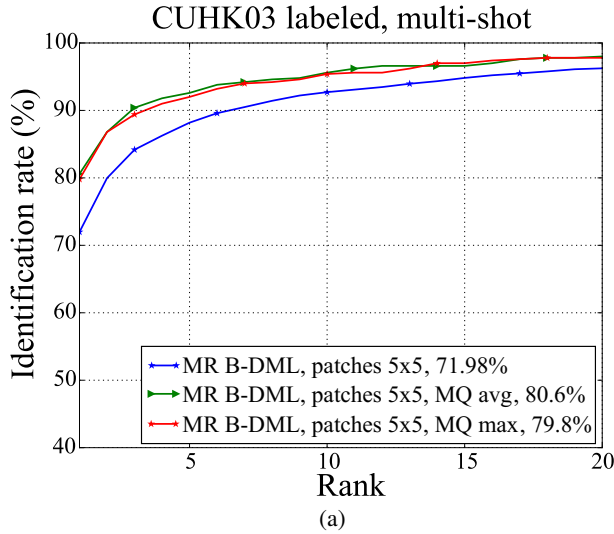


FIG. 5: Results (CMC) of multi-shot experiments for CUHK03 (a) - labeled, (b) - detected. Comparison for query pooling techniques for Multiregion Bilinear DML network. Using multiple queries shows much better results than using only one image for query. Average pooling is slightly better than max pooling for CUHK03.

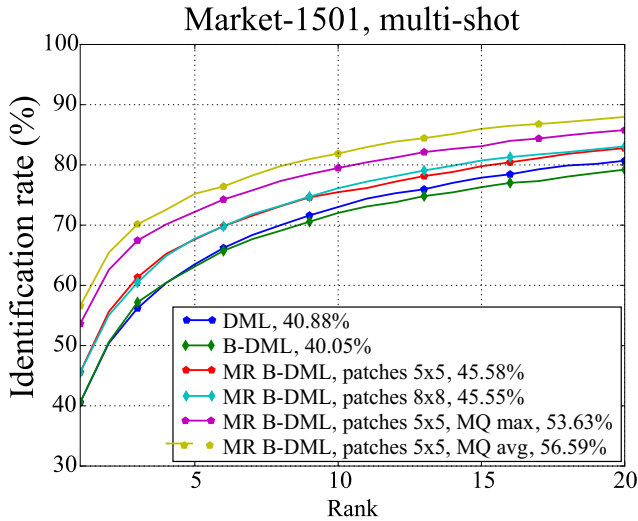


FIG. 6: Results (CMC) of multi-shot experiments for Market-1501. DML architecture is compared with the B-DML and MR B-DML. Multiple queries pooling strategies are also presented.

F. Comparison with the state-of-the-art methods

To our knowledge, Multiregion Bilinear DML networks outperform previously published methods on the CUHK03 dataset (figure 3). The Market-1501 dataset is relatively new and there is only one paper [15] reporting re-identification results for it. We include its best results for the multi-query approach with max-pooling strategy into the final table I. Rank-1 accuracies of the methods are listed in Table I alongside with our results. Follow-

ing [15], we include mean average precision for the experiments on Market-1501.

There are also some negative results that we have encountered. In particular, we have done several experiments with smaller datasets (such as VIPeR [24]) and there we found the baseline DML method to outperform all the bilinear variants. We attribute these results to the small amount of data available for training.

IV. CONCLUSION

In this paper we demonstrated an application of new Multiregion Bilinear CNN architecture to the problem of person re-identification. Having tried different variants of the bilinear architecture, we showed that such architectures give state-of-the-art performance on larger datasets. In particular, Multiregion Bilinear DML allows to retain some spatial information and to extract more complex features, while increase the number of parameters over the baseline CNN without overfitting. We have demonstrated notable gap between the performance of the Multiregion Bilinear DML CNN and the performance of the standard DML CNN [1].

Acknowledgement: This research is supported by the Russian Ministry of Science and Education grant RFMEFI57914X0071.

Current status: This paper is now under consideration at Pattern Recognition Letters.

REFERENCES

- [1] D. Yi, Z. Lei, S. Z. Li, Deep metric learning for practical person re-identification, arXiv preprint arXiv:1407.4979.
- [2] B. Ma, Y. Su, F. Jurie, Bicov: a novel image representation for person re-identification and face verification, in: British Machine Vision Conference, 2012, pp. 11–pages.
- [3] L. Bazzani, M. Cristani, V. Murino, Sdalf: modeling human ap-

- pearance with symmetry-driven accumulation of local features, in: *Person Re-Identification*, Springer, 2014, pp. 43–69.
- [4] S. Li, M. Shao, Y. Fu, Cross-view projective dictionary learning for person re-identification, in: *Proceedings of the 24th International Conference on Artificial Intelligence*, AAAI Press, 2015, pp. 2155–2161.
 - [5] B. Prosser, W.-S. Zheng, S. Gong, T. Xiang, Q. Mary, Person re-identification by support vector ranking., in: *BMVC*, Vol. 2, 2010, p. 6.
 - [6] C.-H. Kuo, S. Khamis, V. Shet, Person re-identification using semantic color names and rankboost, in: *Applications of Computer Vision (WACV)*, 2013 IEEE Workshop on, IEEE, 2013, pp. 281–287.
 - [7] P. M. Roth, M. Hirzer, M. Köstinger, C. Belezni, H. Bischof, Mahalanobis distance learning for person re-identification, in: *Person Re-Identification*, Springer, 2014, pp. 247–267.
 - [8] M. Hirzer, P. M. Roth, H. Bischof, Person re-identification by efficient impostor-based metric learning, in: *Advanced Video and Signal-Based Surveillance (AVSS)*, 2012 IEEE Ninth International Conference on, IEEE, 2012, pp. 203–208.
 - [9] S. Paisitkriangkrai, C. Shen, A. van den Hengel, Learning to rank in person re-identification with metric ensembles, in: *IEEE Conference on Computer Vision and Pattern Recognition (CVPR’15)*, 2015.
 - [10] B. Ma, Y. Su, F. Jurie, Local descriptors encoded by fisher vectors for person re-identification, in: *Computer Vision–ECCV 2012. Workshops and Demonstrations*, Springer, 2012, pp. 413–422.
 - [11] S. Liao, Y. Hu, X. Zhu, S. Z. Li, Person re-identification by local maximal occurrence representation and metric learning, in: *Proceedings of the IEEE Conference on Computer Vision and Pattern Recognition*, 2015, pp. 2197–2206.
 - [12] W. Li, R. Zhao, T. Xiao, X. Wang, Deepreid: Deep filter pairing neural network for person re-identification, in: *IEEE Conference on Computer Vision and Pattern Recognition (CVPR)*, Columbus, USA, 2014.
 - [13] E. Ahmed, M. Jones, T. K. Marks, An improved deep learning architecture for person re-identification, 2015.
 - [14] S.-Z. Chen, C.-C. Guo, J.-H. Lai, Deep ranking for person re-identification via joint representation learning, *arXiv preprint arXiv:1505.06821*.
 - [15] L. Zheng, L. Shen, L. Tian, S. Wang, J. Wang, Q. Tian, Scalable person re-identification: A benchmark, in: *Computer Vision, IEEE International Conference on*, 2015.
 - [16] Y. LeCun, B. E. Boser, J. S. Denker, D. Henderson, R. E. Howard, W. E. Hubbard, L. D. Jackel, Handwritten digit recognition with a back-propagation network, in: *Advances in Neural Information Processing Systems 2*, [NIPS Conference, Denver, Colorado, USA, November 27–30, 1989], 1989, pp. 396–404.
 - [17] R. Zhao, W. Ouyang, X. Wang, Person re-identification by saliency learning, *arXiv preprint arXiv:1412.1908*.
 - [18] A. R. Tsung-Yu Lin, S. Maji, Bilinear cnn models for fine-grained visual recognition, in: *International Conference on Computer Vision (ICCV)*, 2015.
 - [19] A. RoyChowdhury, T.-Y. Lin, S. Maji, E. Learned-Miller, Face identification with bilinear cnns, *arXiv preprint arXiv:1506.01342*.
 - [20] M. Koestinger, M. Hirzer, P. Wohlhart, P. M. Roth, H. Bischof, Large scale metric learning from equivalence constraints, in: *Computer Vision and Pattern Recognition (CVPR)*, 2012 IEEE Conference on, IEEE, 2012, pp. 2288–2295.
 - [21] A. Mignon, F. Jurie, Pcca: A new approach for distance learning from sparse pairwise constraints, in: *Computer Vision and Pattern Recognition (CVPR)*, 2012 IEEE Conference on, IEEE, 2012, pp. 2666–2672.
 - [22] D. J. Jobson, Z.-u. Rahman, G. Woodell, et al., A multiscale retinex for bridging the gap between color images and the human observation of scenes, *Image Processing, IEEE Transactions on* 6 (7) (1997) 965–976.
 - [23] W. Li, R. Zhao, X. Wang, Human reidentification with transferred metric learning., in: *ACCV* (1), 2012, pp. 31–44.
 - [24] D. Gray, S. Brennan, H. Tao, Evaluating appearance models for recognition, reacquisition, and tracking, in: *Proc. IEEE International Workshop on Performance Evaluation for Tracking and Surveillance (PETS)*, Vol. 3, Citeseer, 2007.
 - [25] J. Bromley, J. W. Bentz, L. Bottou, I. Guyon, Y. LeCun, C. Moore, E. Säckinger, R. Shah, Signature verification using a siamese time delay neural network, *International Journal of Pattern Recognition and Artificial Intelligence* 7 (04) (1993) 669–688.
 - [26] S. Chopra, R. Hadsell, Y. LeCun, Learning a similarity metric discriminatively, with application to face verification, in: *Computer Vision and Pattern Recognition*, 2005. *CVPR 2005. IEEE Computer Society Conference on*, Vol. 1, IEEE, 2005, pp. 539–546.
 - [27] B. F. Klare, E. Taborsky, A. Blanton, J. Cheney, K. Allen, P. Grother, A. Mah, M. Burge, A. K. Jain, Pushing the frontiers of unconstrained face detection and recognition: Iarpa janus benchmark a, *algorithms* 13 (2015) 4.
 - [28] S. Lazebnik, C. Schmid, J. Ponce, Beyond bags of features: Spatial pyramid matching for recognizing natural scene categories, in: *2006 IEEE Computer Society Conference on Computer Vision and Pattern Recognition (CVPR 2006)*, 17–22 June 2006, New York, NY, USA, 2006, pp. 2169–2178.
 - [29] P. F. Felzenszwalb, R. B. Girshick, D. McAllester, D. Ramanan, Object detection with discriminatively trained part-based models, *Pattern Analysis and Machine Intelligence, IEEE Transactions on* 32 (9) (2010) 1627–1645.
 - [30] P. Luo, X. Wang, X. Tang, Pedestrian parsing via deep compositional network, in: *Computer Vision (ICCV)*, 2013 IEEE International Conference on, IEEE, 2013, pp. 2648–2655.
 - [31] G. Overett, L. Petersson, N. Brewer, L. Andersson, N. Pettersson, A new pedestrian dataset for supervised learning, in: *Intelligent Vehicles Symposium*, 2008 IEEE, IEEE, 2008, pp. 373–378.

Appendix A: Supplementary material

Here we give the details for the experiments with different initializations of the Bilinear DML architecture. We have observed that initialization with the parameters of the DML network gives the best results.

We have investigated various ways to initialize the B-DML network. Following the intuition behind B-CNN that suggests that the two halves of the network should play different roles (e.g. parts detector and texture descriptor), we tried different initializations for B-CNN feature extractors to find the optimal configuration³. We have always initialized one of the halves of the B-CNN with the baseline DML network, and for the other half we have considered the following options:

- re-identification – the other half is initialized to the same state as the first one using the DML network.
- segmentation – the other half is initialized by the weights of a pretrained semantic segmentation network that used a pixel-wise softmax loss and was trained on Pedestrian Parsing in Surveillance Scenes Dataset (PPSS) [30] (which has 8 class labels corresponding to body parts, and

³ In a sequel, that the same kind two feature extractors are taken for each of three parallel streams.

1,908 images that we downsampled to match the size of the second convolutional layer output in our architecture).

- random – the other half is initialized with random weights.
- detection – the other half is initialized using weights of a trained binary classifier which predicts the presence of pedestrian in the image (binary classification: pedestrian/background). We used NICTA Pedestrian Dataset [31] dataset for training and added CUHK03 training images to enlarge number of images of positive class in the training set. We thus used 200,000 negative images, 37,344 positive images from NICTA and also 11,235 images from CUHK03. After pretraining we took the convolutional layers of the resulting network.

The CMC comparisons of various initialization choices are shown in figure 7. The experiments showed that initializing both feature extractors with weights of the baseline DML is more effective than other initialization schemes both for the labeled and the detected variants of the CUHK03 dataset. This is the initialization strategy that we use in the subsequent experiments.

Interestingly, for the CUHK03-labeled dataset, the baseline DML network outperformed all plain bilinear variants, while for the CUHK03-detected version the situation was reversed. This confirms that the latter scenario is more beneficial for the bilinear networks due to their ability to handle pose variations and/or lack of registration.

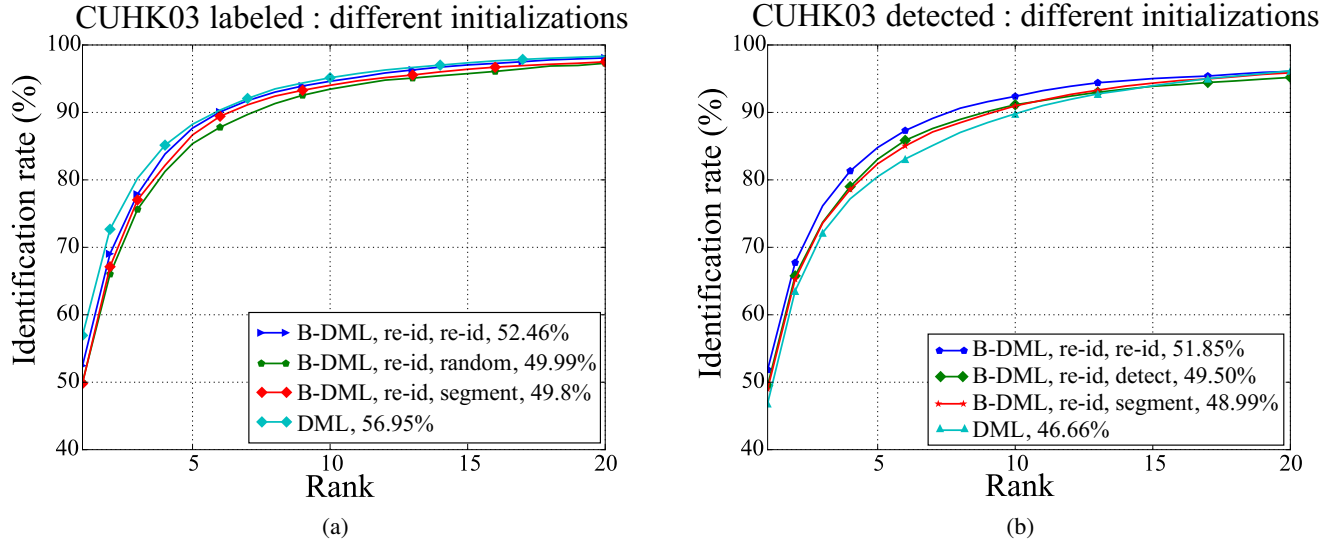


FIG. 7: Single-shot results (CMC) for different initializations of “plain” (i.e. single region) bilinear architecture achieved on (a) - CUHK03-labeled, (b) - CUHK03-detected. After the name of the method, the initialization is indicated. “Re-id” means that one of two feature extractors for bilinear combination is initialized by weights of baseline DML net learned on the same data; “random” means that one of the two feature extractors is initialized randomly; “segment” means that one of the two feature extractors is initialized by the weights of semantic segmentation CNN, “detect” means that one of the two feature extractors is initialized by the weights of the network trained to classify images into “pedestrians” and “non-pedestrians”. Symmetric initialization with the same initialization for both B-CNN halves by the baseline re-identification CNN shows better results than other variants of B-CNN.